Observation of temperature-independent internal Er^{3+} relaxation efficiency in Si-rich SiO_2 films

Oleksandr Savchyn,[1,a)] Ravi M. Todi,[2] Kevin R. Coffey,[2,b)] and Pieter G. Kik[1,b)]
[1]*CREOL, The College of Optics and Photonics, University of Central Florida, 4000 Central Florida Blvd., Orlando, Florida 32816, USA*
[2]*Advanced Materials Processing and Analysis Center (AMPAC), University of Central Florida, 4000 Central Florida Blvd., Orlando, Florida 32816, USA*

(Received 20 February 2009; accepted 30 May 2009; published online 18 June 2009)

Time-dependent photoluminescence measurements of low-temperature-annealed Er-doped Si-rich SiO_2 were conducted at sample temperatures 15–300 K. The erbium internal relaxation efficiency from the second ($^4I_{11/2}$) to the first ($^4I_{13/2}$) excited state upon luminescence-center-mediated Er^{3+} excitation is investigated. Despite the observation of temperature-dependent relaxation rates, the erbium internal relaxation efficiency is found to be remarkably temperature independent, which suggests that the internal relaxation efficiency is near unity. Internal relaxation is shown to account for 50%–55% of the $^4I_{13/2}$ excitation events in the entire temperature range. These results demonstrate that high pump efficiency and stable operation of devices based on this material will be possible under varying thermal conditions. © *2009 American Institute of Physics*.
[DOI: 10.1063/1.3157135]

Currently a significant amount of work is dedicated to the realization of a silicon-based light source for optical on-chip interconnects.[1–5] The recent discovery of luminescence-center-mediated sensitization of Er^{3+} in Si-rich SiO_2 [6,7] and the presence of Er^{3+} sensitization even in samples containing excess silicon but no Si nanocrystals (NCs)[6–8] open up new opportunities to achieve this goal. The use of Er-doped Si-rich SiO_2 without Si NCs could potentially overcome several challenges, including free carrier absorption,[9,10] NC-related scattering losses,[11] and the low density of sensitized Er^{3+} ions[6] inherent to Er-doped Si-rich SiO_2 with Si NCs. In recent study[12] we demonstrated that the excitation of Er^{3+} in Si-rich SiO_2 without Si NCs likely occurs not only into higher energy levels but also directly into the first excited state ($^4I_{13/2}$). As a result, the first excited state of Er^{3+} is populated via two channels: through direct excitation by Si-related luminescence centers (LCs), and through LC-related excitation into higher lying levels followed by internal relaxation of the Er^{3+} ions to the first excited state. These two excitation pathways account for an approximately equal number of excitation events at $T=15$ K.[12] In the current study we monitor temperature-dependent excitation and relaxation rates of Er^{3+} and demonstrate that the internal relaxation remains an efficient excitation channel up to room temperature.

Er-doped Si-rich SiO_2 films containing 12 at. % excess Si and 0.63 at. % of Er were prepared by magnetron cosputtering onto a Si substrate. The samples were annealed for 100 s in N_2 at 600 °C or 1100 °C (labeled LTA and HTA, respectively, for low and high temperature annealing) and subsequently passivated for 30 min in forming gas (N_2:H_2 =95%:5%) at 500 °C. No Si aggregates could be detected in transmission electron microscopy measurements on LTA samples, while measurements on HTA samples clearly showed the presence of NCs.[6] Optical measurements were performed in a closed-loop He cryostat in the temperature range 15–300 K. Photoluminescence (PL) spectra were taken under 351 nm excitation with a Kr-ion laser (pump irradiance 1.40 W/cm^2). The PL spectra were corrected for the system spectral response. The time-dependent PL signal was measured either under modulated continuous wave (cw) pumping using the excitation parameters described above or using pulsed excitation with the 355 nm line of a neodymium doped yttrium aluminum garnet laser with a pulse width of 5 ns and a pulse energy of 1.9 μJ. All measured PL parameters have an experimental error smaller than ±5%. A more detailed description of the experimental procedures can be found in Refs. 6, 7, and 12.

The PL spectra of the LTA sample shown in Fig. 1(a) exhibit four emission bands: a band peaking at ~600 nm corresponding to the emission from silicon-excess-related LCs,[13] a band peaking at 1128 nm most likely corresponding to radiative exciton recombination in the Si substrate, and two Er-related emission bands at 981 and 1535 nm corresponding to the transitions $^4I_{11/2}\rightarrow{}^4I_{15/2}$ and $^4I_{13/2}\rightarrow{}^4I_{15/2}$, respectively. The PL spectra of the HTA sample shown in Fig. 1(b) exhibit three emission bands: a broad emission band peaking at ~750 nm typically attributed to emission from Si NCs in the Si-rich SiO_2 matrix and the two Er-related emission bands that were also observed in the LTA sample. In both samples the Er-related emission at 1535 nm shows pronounced spectral broadening with increasing temperature due to the temperature-dependent redistribution of the excited states over the Stark-split $^4I_{13/2}$ level. No Er^{3+} emission could be detected in samples containing a similar Er concentration (0.49 at. %) but no Si excess under cw or pulsed excitation. This clearly demonstrates that the excitation of Er^{3+} in the LTA and HTA samples is predominantly indirect and Si-excess related. To ensure similar excitation conditions the measurements under both cw and pulsed excitation were taken at sufficiently low pump power to avoid significant signal saturation and second order processes (cooperative upconversion, excited state absorption).

Based on lifetime measurements at 1535 nm under modulated cw excitation (not shown) the excitation rate of

a)Electronic mail: osavchyn@mail.ucf.edu.
b)Also at Physics Department, University of Central Florida.

 © 2009 American Institute of Physics

Downloaded 19 Jun 2009 to 132.170.51.129. Redistribution subject to AIP license or copyright; see http://apl.aip.org/apl/copyright.jsp

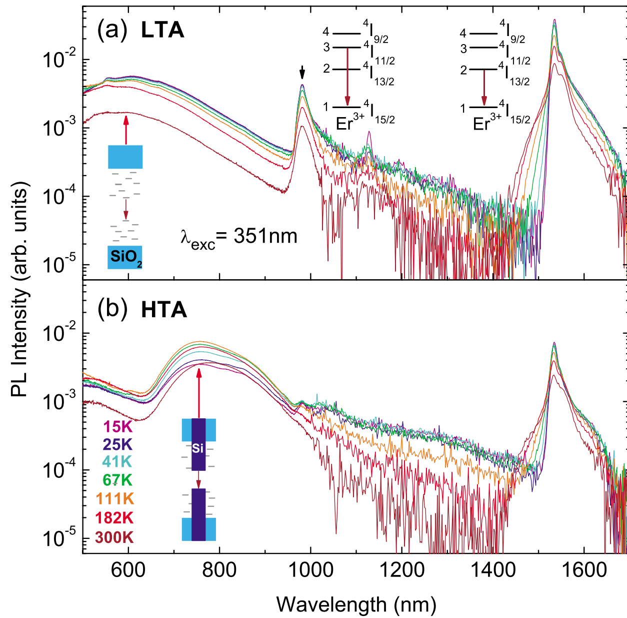

FIG. 1. (Color online) Temperature-dependent photoluminescence spectra of Er-doped Si-rich SiO_2 annealed at 600 °C (LTA) (a) and at 1100 °C (HTA) (b). The corresponding optical transitions are schematically indicated.

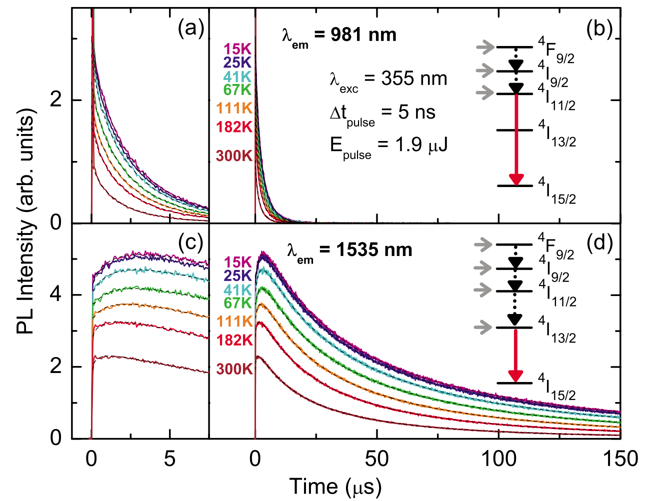

FIG. 3. (Color online) Time-dependent Er^{3+} PL intensity at 981 nm [(a) and (b)] and at 1535 nm [(c) and (d)] under pulsed excitation at 355 nm (solid lines) with the corresponding fits (dashed lines). All intensities are shown on the same relative scale. Contributing excitation channels are schematically indicated by the horizontal and dashed vertical arrows. The relevant optical transitions are indicated by the solid vertical arrows.

the first excited state of Er^{3+} (R_{exc}) in LTA and HTA samples was determined using the well known relation $R_{\mathrm{exc}}=\tau_{\mathrm{rise}}^{-1}-\tau_{\mathrm{dec}}^{-1}$ where τ_{rise} and τ_{dec} are, respectively, the rise and decay times of the emission. The results are shown in Fig. 2(a). Note that despite the significant difference in the stoichiometry of the LTA and HTA samples, the observed excitation rates are similar in value and are both virtually temperature independent. This provides further evidence for a similar origin of Er^{3+} sensitization in these different samples.

Figures 3(a) and 3(b) show the time-dependent PL intensity at 981 nm in the LTA sample taken under pulsed excitation at 355 nm. The excitation of the second excited state was found to take place on a time scale <27 ns at

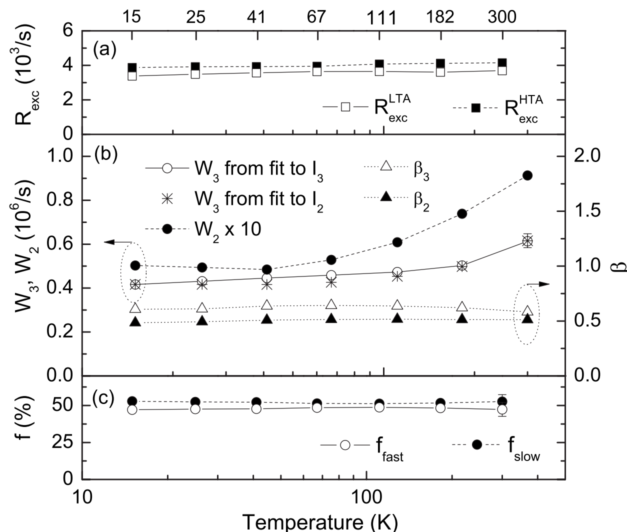

FIG. 2. Temperature dependence of (a) the Er^{3+} first excited state excitation rate in LTA ($R_{\mathrm{exc}}^{\mathrm{LTA}}$) and HTA ($R_{\mathrm{exc}}^{\mathrm{HTA}}$) samples, (b) the Er^{3+} second excited state relaxation rate (W_3) found from the time-dependent intensities at 981 nm (I_3) and 1535 nm (I_2), the first excited state relaxation rate (W_2), and the dispersion factors corresponding to the relaxation from the first (β_2) and second (β_3) excited states, (c) the relative fractions of the first excited state excitation events due to the fast (f_{fast}) and slow (f_{slow}) excitation processes.

all temperatures. The $1/e$ decay times of the second excited state of Er^{3+} ($^4I_{11/2}$) τ_3 were obtained by fitting the measured decay traces with the function $I_3(t)=I_3(0)\times\exp[-(t/\tau_3)^{\beta_3}]$. All decay traces exhibited a temperature-independent value of $\beta_3=0.79+/-0.01$. The corresponding decay rate of the second excited state of Er^{3+} in the LTA sample $W_3=1/\tau_3$ is shown in Fig. 2(b) and demonstrates a gradual increase by a factor of ~1.5 as the temperature is increased from 15 to 300 K.

Figures 3(c) and 3(d) show the time-dependent PL intensity at 1535 nm in the LTA sample taken under pulsed excitation. The shape of these traces results from the presence of two distinct sensitization mechanisms:[12] a fast excitation process taking place on a timescale <27 ns due to excitation of Er^{3+} by LCs apparently directly into the first excited state and a slow excitation process taking place on a timescale of several microseconds due to the LC-mediated excitation of Er^{3+} into higher energy levels followed by relatively slow relaxation to the first excited state. The short time constant (<27 ns) of the fast excitation of both the first and second excited states at all considered temperatures suggests a similar origin of the fast excitation of both states. The experimental decay traces at 1535 nm are described by the function:[12]

$$I_2 \propto N_2^{\mathrm{fast}}(0)e^{-(t/\tau_2)^{\beta_2}}+\frac{N_3(0)}{\tau_{32}(\tau_3^{-1}-\tau_2^{-1})}\left[e^{-(t/\tau_2)^{\beta_2}}-e^{-(t/\tau_3)^{\beta_3}}\right], \quad (1)$$

where $N_2^{\mathrm{fast}}(0)$ and $N_3(0)$ are the densities of the Er^{3+} ions excited by the fast process into the first and higher excited states, respectively, τ_2, β_2 and τ_3, β_3 are the decay times and the dispersion factors, respectively, of the first and second excited states and τ_{32} is the relaxation time from the second to the first excited state of Er^{3+}. The thus obtained $W_3=1/\tau_3$ values are in excellent agreement with the corresponding decay rates acquired from the fit to the time-dependent 981 nm emission [Fig. 2(b)], strongly supporting the presented model. The decay rate of the first excited state ($W_2=1/\tau_2$) of the LTA sample is included in Fig. 2(b) and shows a similar to W_3 increase by a factor of ~1.9. The values of

Downloaded 19 Jun 2009 to 132.170.51.129. Redistribution subject to AIP license or copyright; see http://apl.aip.org/apl/copyright.jsp

the dispersion factors β_2 and β_3 describe the observed multiexponential decay, which is likely caused by the presence of Er^{3+} ions with different decay rates. The obtained dispersion factors are shown in Fig. 2(b), and can be seen to be relatively constant, suggesting that temperature affects all Er^{3+} ions responsible for the emission in a similar manner.

The relaxation rate W_3 is commonly assumed to be dominated by multiphonon relaxation from the second to the first excited state, with the energy difference bridged predominantly by high energy phonons[14] with energies of $\sim 130-150$ meV in the case of SiO_2.[15,16] However, using the well known expression for the multiphonon relaxation rate,[14] the temperature dependence of W_3 could not be accurately described. This suggests that a non-phonon-related temperature-dependent nonradiative decay channel is present. This assumption is supported by the room temperature relaxation rate of $W_3 = 6.2 \times 10^5$ s^{-1}, which is much larger than both the room temperature multiphonon rate of $\sim 1 \times 10^5$ s^{-1} (Ref. 14) and the typical radiative rate of $\sim 100-130$ s^{-1} (Ref. 17) of the second excited state of Er^{3+} in silicate glasses. Note that the first excited state decay rate W_2, which is known to be approximately temperature independent in SiO_2 (Ref. 17) also increases by a factor of ~ 1.9 in this temperature range. Both observations are likely due to the presence of nonradiative relaxation through coupling with low-energy electronic transitions in this low-temperature processed Si-doped oxide. This suggests that the technical implementation of this material requires thermal processing that minimizes the presence of electronic defects, while avoiding the formation of extended Si NCs.

The temperature dependence of the fractions of Er^{3+} ions excited into the first excited state via the fast (f_{fast}) and slow (f_{slow}) process, respectively, found from the time integration of the first and second terms in Eq. (1) (Ref. 12) is shown in Fig. 2(c). Surprisingly, for all temperatures the fast and slow excitation mechanisms are responsible for 45%–50% and 50%–55%, respectively, of the excitation events into the first excited state. Assuming that the fast excitation of the first and second excited states have the same temperature dependence, the observed temperature-independent contribution of each of the excitation pathways of the first excited state suggests that the relaxation efficiency from the second to the first excited state of Er^{3+} (η_{32}) does not change significantly with temperature. However, the total relaxation rate from the second excited state (W_3) does vary with temperature by a factor of ~ 1.5, increasing from 4.2×10^5 s^{-1} at 15 K to 6.2×10^5 s^{-1} at room temperature [Fig. 2(b)]. Since $W_3 = W_{32} + W_{31}$ where $W_{32} = 1/\tau_{32}$ is the relaxation rate from the second to the first excited state and W_{31} is the relaxation rate from the second excited state to the ground state, this increase in W_3 indicates that at least one of the two contributing relaxation rates W_{32} and W_{31} increases with temperature. This in turn would lead to a temperature-dependent relaxation quantum efficiency from the second to the first excited state given by $\eta_{32} = W_{32}/W_3 = (1 + W_{31}/W_{32})^{-1}$, which would be accompanied by a change of the excitation rate of the first excited state (R_{exc}), and a change of the relative fraction of Er^{3+} ions excited into the first excited state by the slow excitation mechanism (f_{slow}). Based on the fact that neither of these changes are observed we conclude that the relaxation efficiency is temperature independent.

The temperature independent relaxation efficiency can be explained by assuming a relatively slow relaxation from the second excited state to the ground state ($W_{31} \ll W_{32}$ and thus $W_3 = W_{32} + W_{31} \approx W_{32}$) resulting in $W_{31}/W_{32} \ll 1$. Under this assumption and realizing that $\eta_{32} = W_{32}/W_3 = (1 + W_{31}/W_{32})^{-1}$ we find $\eta_{32} \approx 1$. Alternatively the temperature independent relaxation efficiency could be explained by assuming an identical temperature dependence of W_{32} and W_{31}. This scenario is considered unlikely due to the significantly different energy of the ${}^4I_{11/2} \rightarrow {}^4I_{15/2}$ and ${}^4I_{11/2} \rightarrow {}^4I_{13/2}$ transitions (1.26 and 0.45 eV, respectively). Based on these considerations it seems most likely that the decay from the second excited state is dominated by the relaxation to the first excited state ($W_3 \approx W_{32}$), suggesting that the relaxation efficiency η_{32} in this material is near-unity.

In summary, luminescence-center-mediated Er^{3+} excitation is shown to occur with near-equal probability through direct excitation into the first excited state (45%–50%) and through excitation into higher levels followed by relaxation to the first excited state (50%–55%) in the entire temperature range 15–300 K. The observation of a temperature-independent Er^{3+} excitation rate and a temperature-independent fraction of Er^{3+} excitation events occurring via the second excited state combined with the observed increasing second excited state relaxation rate suggests a constant near-unity relaxation efficiency from the second to the first excited state of Er^{3+} in low-temperature-annealed Er-doped Si-rich SiO_2 in this temperature range. These results indicate that high pump efficiency and stable room temperature operation of devices based on this material are possible.

This work was supported by the National Science Foundation CAREER No. ECCS-0644228.

[1]M. Lipson, J. Lightwave Technol. **23**, 4222 (2005).
[2]M. Makarova, V. Sih, J. Warga, R. Li, L. Dal Negro, and J. Vuckovic, Appl. Phys. Lett. **92**, 161107 (2008).
[3]L. Dal Negro, R. Li, J. Warga, and S. N. Basu, Appl. Phys. Lett. **92**, 181105 (2008).
[4]Q. Lin, T. J. Johnson, R. Perahia, C. P. Michael, and O. J. Painter, Opt. Express **16**, 10596 (2008).
[5]T. J. Kippenberg, J. Kalkman, A. Polman, and K. J. Vahala, Phys. Rev. A **74**, 051802 (2006).
[6]O. Savchyn, F. R. Ruhge, P. G. Kik, R. M. Todi, K. R. Coffey, H. Nukala, and H. Heinrich, Phys. Rev. B **76**, 195419 (2007).
[7]O. Savchyn, P. G. Kik, R. M. Todi, and K. R. Coffey, Phys. Rev. B **77**, 205438 (2008).
[8]G. Franzò, S. Boninelli, D. Pacifici, F. Priolo, F. Iacona, and C. Bongiorno, Appl. Phys. Lett. **82**, 3871 (2003).
[9]D. Navarro-Urrios, A. Pitanti, N. Daldosso, F. Gourbilleau, R. Rizk, G. Pucker, and L. Pavesi, Appl. Phys. Lett. **92**, 051101 (2008).
[10]R. D. Kekatpure and M. L. Brongersma, Nano Lett. **8**, 3787 (2008).
[11]R. D. Kekatpure and M. L. Brongersma, Phys. Rev. A **78**, 023829 (2008).
[12]O. Savchyn, R. M. Todi, K. R. Coffey, and P. G. Kik, Appl. Phys. Lett. **93**, 233120 (2008).
[13]M. Ya. Valakh, V. A. Yukhimchuk, V. Ya. Bratus, A. A. Konchits, P. L. F. Hemment, and T. Komoda, J. Appl. Phys. **85**, 168 (1999).
[14]C. B. Layne, W. H. Lowdermilk, and M. J. Weber, Phys. Rev. B **16**, 10 (1977).
[15]F. L. Galeener and G. Lucovsky, Phys. Rev. Lett. **37**, 1474 (1976).
[16]C. T. Kirk, Phys. Rev. B **38**, 1255 (1988).
[17]E. Desurvire, *Erbium-doped Fiber Amplifiers: Principles and Applications* (Wiley, Hoboken, New Jersey, 2002), Chap. 4, pp. 223–224.

Downloaded 19 Jun 2009 to 132.170.51.129. Redistribution subject to AIP license or copyright; see http://apl.aip.org/apl/copyright.jsp